analytical chemistry

pubs.acs.org/ac Article

Antigen-Down PEC Immunosensor for CYFRA21-1 Detection Based on Photocurrent Polarity Switching Strategy

Jinhuan Zhang, Xiaodong Xue, Yizhen Du, Jinxiu Zhao, Hongmin Ma, Xiang Ren,* Qin Wei, and Huangxian Ju

Cite This: https://doi.org/10.1021/acs.analchem.2c01478 Read Online

ACCESS | Metrics & More | Article Recommendations | Supporting Information

ABSTRACT: In this work, an antigen-down photoelectrochemical (PEC) immunosensor based on a signal polarity switching strategy for the detection of cytokeratin 19 fragment 21-1 (CYFRA21-1) was proposed. 3,4,9,10-Perylene tetracarboxylic acid (PTCA) is a conjugated organic dye containing five benzene nuclei, which has excellent film-forming and optical properties. PTCA sensitized by SnS_2 can further improve the basal signal and the stability of the PEC immunosensor. Moreover, avidin-functionalized $CuInS_2$ as a signal probe can convert the basal anodic photocurrent to a cathodic photocurrent. Therefore, the PEC sensor realized the photocurrent polarity conversion before and after labeling. With avidin-functionalized $CuInS_2$, the polarity of the photocurrent was changed once CYFRA21-1 was detected. Therefore, the PEC immunosensor owns high sensitivity. The linear range of the immunosensor for the detection of CYFRA21-1 is 0.00001−500 ng·mL^{-1}, and the detection limit is 3.5 fg·mL^{-1}. The PEC immunosensor has good stability, high selectivity, and good repeatability. This work may provide a new way for the detection of CYFRA21-1 and other proteins.

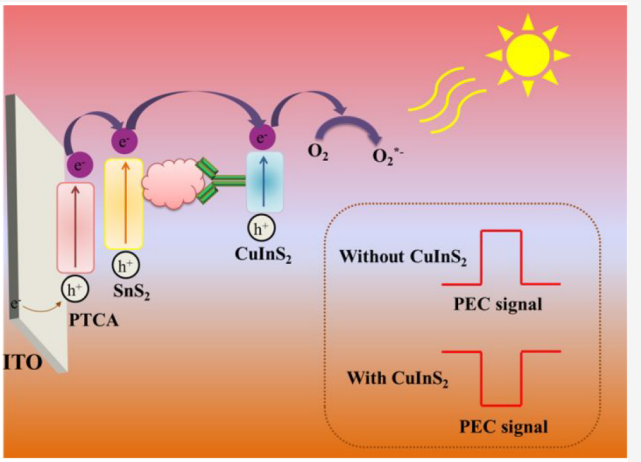

1. INTRODUCTION

Lung cancer is one of the malignant tumors with fast-growing morbidity and mortality, posing a great threat to people's health and life, and it remains the leading cause of cancer-related death in the world.[1,2] Non-small cell carcinoma is a kind of lung cancer, accounting for about 80% of lung cancer.[3] Therefore, it is of great significance to monitor non-small cell carcinoma. Cytokeratin 19 fragment 21-1 (CYFRA21-1) is the most valuable tumor marker of non-small cell carcinoma. A concentration of CYFRA21-1 in human serum higher than 3.5 ng·mL^{-1} is considered abnormal.[4,5] Up to now, there have been many techniques for detecting cancer markers, such as electrochemistry,[6−8] electrochemiluminescence,[9,10] and fluorescence.[11−13] Because the expensive instruments and complex operating steps severely restrict development of these techniques, it is necessary to find a highly sensitive, low cost, and simple technique for the detection of CYFRA21-1. As an innovative immunoassay platform, a photoelectrochemical (PEC) immunosensor has the advantages of low background signal, low cost, easy miniaturization, high sensitivity, and specificity in detecting CYFRA21-1.[14−16] All in all, it is of great significance to construct a sensitive PEC immunosensor for CYFRA21-1 detection.

A PEC immunosensor is mainly used to detect antigen (Ag) and antibody (Ab) by chemical methods.[17,18] Substrate photosensitive material is an indispensable component of the photoelectrochemical immunosensor, so it is necessary to seek stable and nontoxic materials with good photoelectric properties. 3,4,9,10-Perylene tetracarboxylic acid (PTCA) is a sheetlike organic photosensitizer with a pentaphenyl nucleus and has excellent photoelectric properties and film-forming ability;[19] thus it is used as an ideal photoelectric material for constructing a PEC immunosensor. However, PTCA has a narrow band gap energy (~2.2 eV),[20] which leads to the easy recombination of photogenerated electrons (e^-) and holes (h^+). The method to solve this problem is to use SnS_2 with an excellent performance for sensitization. A possible mechanism for this sensitization method can be explained as follows: when light is excited, electrons in the conduction band (CB) of

Received: April 5, 2022
Accepted: August 22, 2022

Downloaded via NANJING UNIV on September 2, 2022 at 12:52:48 (UTC).
See https://pubs.acs.org/sharingguidelines for options on how to legitimately share published articles.

ACS Publications © XXXX American Chemical Society

https://doi.org/10.1021/acs.analchem.2c01478
Anal. Chem. XXXX, XXX, XXX−XXX

Scheme 1. Possible Photogeneration Electron Transfer Mechanisms at (A) SnS_2/PTCA/ITO and (B) Avidin-$CuInS_2$/Ab-Biotin/BSA/Ag/EDC-NHS/TGA/SnS_2/PTCA/ITO

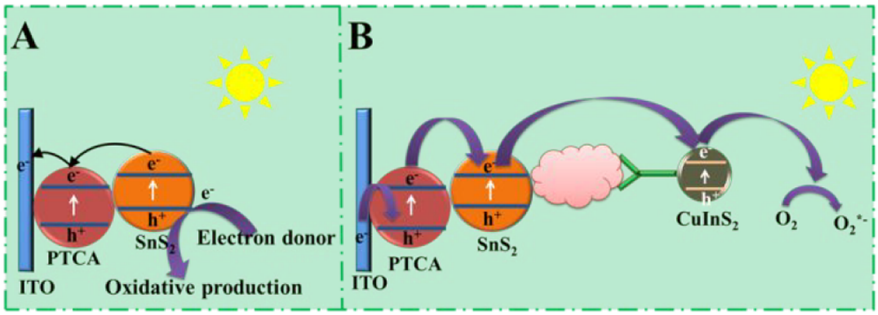

SnS_2[21,22] can be transferred to the CB of PTCA, thus improving the photoelectric conversion efficiency.

Meanwhile, it is vital to find a sensitive strategy for construction of a PEC immune platform. At present, most of the reported photoelectrochemical immunosensors are based on the detection strategy that the polarity of the photocurrent does not change before and after labeling, but this detection strategy has some disadvantages. For conventional signal-off and signal-on sensors, the direction of the photocurrent does not change with the concentration of the target. For the former, when the target molecule concentration reaches a certain value, the photocurrent cannot decrease with the increase of the target molecule concentration. This limits the detection limit of the sensor.[23,24] Moreover, the different photocurrent directions of the constructed sensor and the base photosensitive material can eliminate false positive and false negative detection results to a certain extent. Therefore, a PEC sensor based on the polarity switching strategy can have a larger detection limit and better anti-interference ability.

In this work, a highly sensitive detection method of CYFRA21-1 based on the polarity conversion of photocurrent before and after labeling is proposed for the first time, and the above problems can be effectively avoided. SnS_2 sensitized PTCA could produce a stable and large anodic photocurrent as the basal material. $CuInS_2$, as a ternary p-type semiconductor photosensitive material, has the advantages of a high light absorption coefficient and low toxicity.[25,26] It is generally accepted by researchers that photosensitive materials are irradiated with internal electrons due to the transition from the valence band (VB) to the CB. The possible mechanism of the change of the photocurrent signal before and after labeling is the following. In this work, the photoexcited electrons of SnS_2 and PTCA transition from the VB to the CB. Due to the appropriate band gap matching, the electrons can transmit from the CB of SnS_2 to the CB of PTCA and the ITO electrode. At the same time, the holes in the VB of SnS_2 and PTCA can consume the electrons provided by the electron donors in the solution. The electrons can move from the electrolyte solution to the ITO electrode, resulting in an anodic current (Scheme 1A). However, when the marker $CuInS_2$ is introduced into the ITO electrode surface, $CuInS_2$ plays a leading role on the sensor surface. Electrons transition from the VB to the CB of photosensitive materials, and most of the electrons are transferred from the electrode to the VB of PTCA, further to the CB of SnS_2, and then to the CB of $CuInS_2$. Finally, the electron acceptor in the solution is captured. The electrons move from the ITO electrode to the electrolyte solution, resulting in a cathodic current (Scheme 1B). The avidin−biotin immobilization process involves merely a single attachment point of the biomolecules, thus facilitating a recognition phenomenon such as immunoreaction.[27] Avidin-$CuInS_2$ is used as the marker, and Ab-biotin is an antibody linked with biotin. The major distinguishing feature of the avidin−biotin connection is the extraordinary affinity, which provides an effective method for connecting Ab and markers. Moreover, the fixation process of avidin linked with biotin only involves a single attachment point of biomolecules, which is beneficial to an immune reaction. At the same time, the identification of markers and antigens is accomplished by the specific identification of avidin and biotin, which greatly improves the sensitivity of immunosensor. The strategy realizes the conversion of photocurrent polarity before and after marking. In general, the sensor constructed that uses PTCA as the base material switches the photocurrent polarity before and after the avidin-$CuInS_2$ labeling, so that a greater detection limit can be obtained. The construction process of the immunosensor is shown in Scheme 2.

Scheme 2. Fabrication Process of Proposed Photoelectrochemical Immunosensor

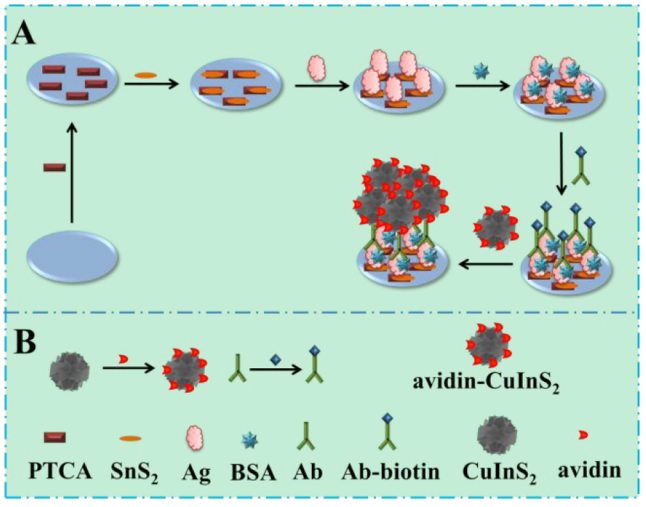

2. EXPERIMENTAL SECTION

Preparation of Avidin-$CuInS_2$. The preparation of $CuInS_2$ was according to the simple hydrothermal method shown in the Supporting Information. Briefly, the prepared $CuInS_2$ (50 mg) was dispersed in a mixed solvent consisting of 47.5 mL of ethanol and 2.5 mL of water. Next, $CuInS_2$

https://doi.org/10.1021/acs.analchem.2c01478
Anal. Chem. XXXX, XXX, XXX−XXX

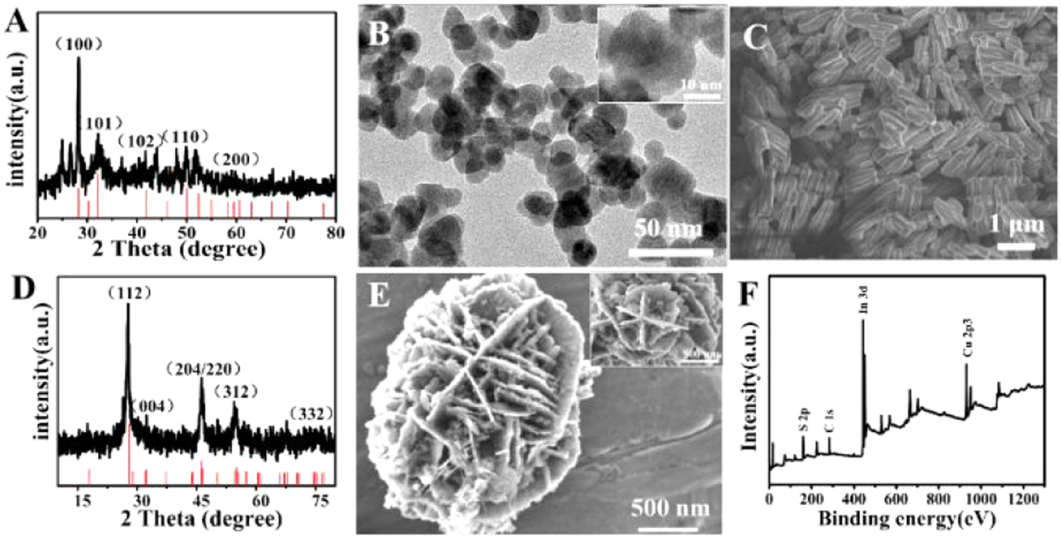

Figure 1. (A) XRD pattern and (B) SEM image of SnS_2. (C) SEM image of PTCA. (D) XRD pattern and (E) SEM image of $CuInS_2$. (F) X-ray photoelectron spectrum of $CuInS_2$.

suspension liquid was added to 1 mL of APTES, and the mixed suspending liquid was ultrasonicated for 20 min. After that, it was heated at 75 °C for 1 h. Then, the suspending liquid was washed with ethanol three times and dried at 60 °C to get amino-functionalized $CuInS_2$. The prepared amino-functionalized product (10 mg) was dispersed in 2 mL of Tris-HCl (pH 7.4) buffer. Then, 400 μL of glutaraldehyde solution (2.5 wt %) was injected into the suspension and incubated for 2 h at room temperature. After it was washed, the obtained mixture was dispersed in 1 mL of Tris-HCl (pH 7.4) buffer solution. Afterward, 100 μL of avidin (1 mg·mL^{-1}) was added to the above suspension and the suspension was incubated at 4 °C for 1 h. Finally, after it was washed, it was redispersed in 2 mL of Tris-HCl (pH 7.4, containing 1 wt % BSA) to obtain avidin-$CuInS_2$.

Preparation of Ab-Biotin. First, 10 μL of EDC/NHS solution (EDC 5 mg·mL^{-1}, NHS 1 mg·mL^{-1}) was dispersed in 1 mL of Ab (1 μg·mL^{-1}) solution, and then 200 μL of biotin hydrazide (1 mg·mL^{-1}) solution was added. The obtained solution was shocked at room temperature for 2 h and then stored in a refrigerator at 4 °C for standby.

Fabrication of PEC Sensor. The size of the ITO glass electrode is 0.8 × 2.0 cm^2. ITO electrodes were washed and dried before modification. First of all, 10 μL of PTCA solution (5 mg·mL^{-1}) was dropped onto the ITO electrode and dried at room temperature to obtain the PTCA-modified electrode. The PTCA/ITO electrode was then modified with 10 μL of SnS_2 solution (5 mg·mL^{-1}). Following the same procedure, the electrode was modified with 3 μL of TGA solution (3 mmol·L^{-1}) and 3 μL of mixed solution (containing 5 mg·mL^{-1} EDC and 1 mg·mL^{-1} NHS) at room temperature to obtain TGA/SnS_2/PTCA/ITO and EDC-NHS/TGA/SnS_2/PTCA/ITO electrodes. Then, 4 μL of CYFRA21-1 (0.00001−500 ng·mL^{-1}) solution was added dropwise to the electrode and incubated at 4 °C for 40 min to obtain the Ag/EDC-NHS/TGA/SnS_2/PTCA/ITO electrode. The electrodes were then modified with 3 μL of BSA (1 wt %) to block nonspecific active sites. The electrodes were incubated with 4 μL of Ab-biotin solution for 40 min at 4 °C. Until it was washed, the electrode was incubated with 4 μL of avidin-$CuInS_2$ for 40 min. Finally, the electrode was rinsed with Tris-HCl (pH 7.4) buffer solution and was ready to be used for PEC measurements.

PEC Measurement. The photocurrent was measured on a photoelectrochemical workstation (CHI 760E Chenhua Instrument Co., Shanghai, China). A Ag/AgCl electrode and a platinum electrode were used as the reference electrode and the counter electrode, respectively, and detection was carried out in Tris-HCl (pH 7.4) buffer solution. An LED lamp (450 nm) was used as the excitation light, and it was switched every 10 s at 0 V (vs Ag/AgCl) potential.

3. RESULTS AND DISCUSSION

Characterization of Synthesized Materials. Figure 1A shows the XRD pattern of synthesized SnS_2 powder, which accords with that of SnS_2 (JCPDS 23-0677). Figure 1B shows that SnS_2 is in nanosheets with a diameter of about 20 nm. This indicates that SnS_2 nanosheets have been successfully prepared. In Figure 1C, the SEM image of PTCA shows a short rodlike appearance, which is consistent with the literature report. An XRD pattern consistent with $CuInS_2$ is shown in Figure 1D, which is in conformity with JCPDS 27-0159. The observed peaks belong to (112), (004), (204/220), (312), and (332) crystals. Figure 1E shows an SEM image of $CuInS_2$. It can be seen that the sample is a floret about 2 μm in size. It can be observed that these microflowers are composed of plates with large specific surface areas, which provide more areas for photogenerated electrons. In order to study the chemical valence and surface chemical environment of the sample, $CuInS_2$ was studied by XPS. As shown in Figure 1F, for the peaks of four main elements, including S, In, Cu, and C, the binding energy of S 2p is about 160−161.5 eV and the 2p orbital of Cu is divided into two peaks (950.35 and 930.6 eV), which respectively refer to Cu^+. The peak intensities of In are at 444.6 and 452.3 eV, pointing to In $3d_{5/2}$ and In $3d_{3/2}$, respectively. Therefore, it has been proved that $CuInS_2$ was successfully synthesized.

Possible PEC Mechanism of Immunoassay. The electron transfer process in the Tris-HCl (7.4) buffer solution was expected to be as described below. PTCA has a narrow band gap, e^- and h^+ are easy to recombine, and SnS_2 has a matching energy level with it. Inhibition of recombination can

https://doi.org/10.1021/acs.analchem.2c01478
Anal. Chem. XXXX, XXX, XXX−XXX

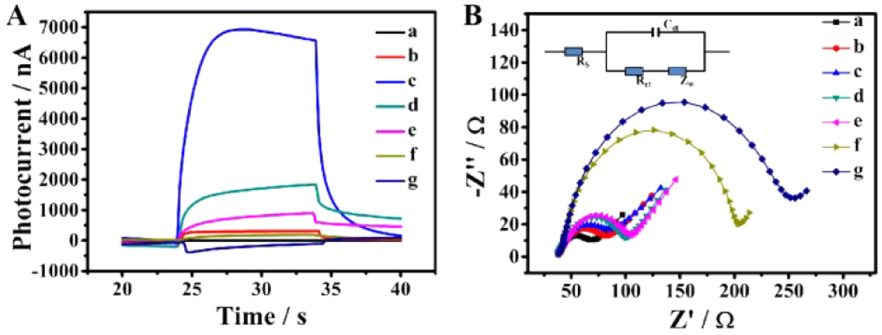

Figure 2. (A) PEC signal responses and (B) EIS results of (a) unmodified ITO electrode, (b) PTCA/ITO, (c) SnS_2/PTCA/ITO, (d) Ag/EDC-NHS/TGA/SnS_2/PTCA/ITO, (e) BSA/Ag/EDC-NHS/TGA/SnS_2/PTCA/ITO, (f) Ab-biotin/BSA/Ag/EDC-NHS/TGA/SnS_2/PTCA/ITO, and (g) avidin-$CuInS_2$/Ab-biotin/BSA/Ag (0.5 ng·mL^{-1}) EDC-NHS/TGA/SnS_2/PTCA/ITO. (B, inset) Electrical equivalent circuit applied to fit the impedance spectra.

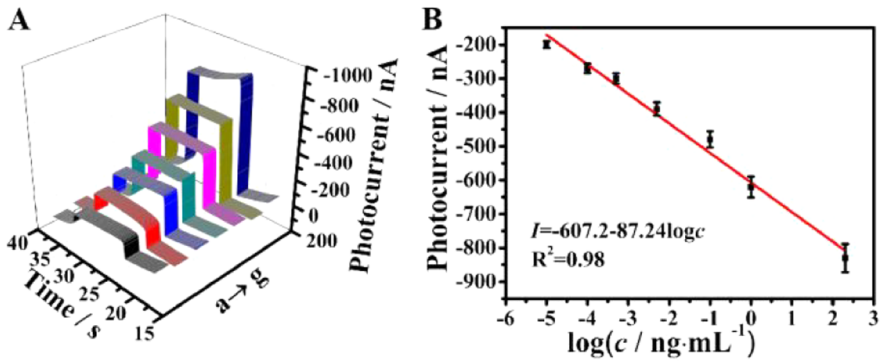

Figure 3. (A) Photocurrent response and (B) homologous fitting curve of avidin-$CuInS_2$/Ab-biotin/BSA/Ag/EDC-NHS/TGA/SnS_2/PTCA/ITO electrode in the presence of 3 μL of different concentrations of Ag: (a) 0.00001, (b) 0.0005, (c) 0.0001, (d) 0.005, (e) 0.1, (f) 1, and (g) 200 ng·mL^{-1}. This results were tested in Tris-HCl buffer solution (pH 7.4). Error bars = SD (n = 3).

increase the photocurrent and improve the stability of the photoelectrochemical immunosensor. Avidin-$CuInS_2$ was used as a marker to change the polarity of the photocurrent. It could reduce the interference of the background signal and improve the sensitivity of the PEC immunosensor. SnS_2/PTCA/ITO was illuminated, and photogenerated electrons were transferred from the CB of PTCA to ITO, which reduced the recombination of e^- and h^+ and produced an anodic photocurrent. For avidin-$CuInS_2$/Ab-biotin/BSA/Ag/EDC-NHS/TGA/SnS_2/PTCA/ITO electrodes, photoelectrons are transferred from the CB of PTCA to the CB of SnS_2 and further to the CB of $CuInS_2$ (Scheme 1). Then the electrons at the conduction band of $CuInS_2$ are consumed by the dissolved oxygen in the electrolyte solution, thus generating a cathodic photocurrent. Avidin-$CuInS_2$, as a polarity conversion element, produced a photocurrent with opposite polarity before and after labeling, which improved the sensitivity of the PEC immunosensor. Therefore, an immunosensor of photocurrent polarity conversion before and after marker labeling was successfully constructed.

Characterization of the PEC Immunosensor. By modifying the ITO electrode layer by layer with different materials, the photocurrent was detected. As shown in Figure 2A, the photocurrent detected by the bare ITO can almost be ignored (curve a). With the modification of PTCA (curve b), the value of photocurrent increased further. With the modification of SnS_2 (curve c), the photocurrent value reached the maximum at this time. With the subsequent modification of Ag (curve d) at a concentration of 0.05 mg·mL^{-1}, BSA (curve e), and Ab-biotin (curve f) with great impedance, the photocurrent value gradually decreased. After the modification of the last layer of avidin-$CuInS_2$ (curve g), because avidin-$CuInS_2$ was a photocathode material, it produced a cathodic photocurrent with the opposite polarity to the photocurrent of the previous modified layer; thus the above showed that this sensor was perfectly modified.

At the same time, electrochemical impedance spectroscopy (EIS) was used to prove that the electrode layer was successfully modified. As shown in Figure 2B, the bare ITO glass electrode (curve a) showed a small resistance. The successive increase in impedance values of curves a and b is due to the sequential modification of the semiconductor PTCA and SnS_2. When the electrode was modified with Ag (curve d), BSA (curve e), Ab-biotin (curve f), and avidin-$CuInS_2$ (curve g) in turn, the radius of the semicircle increased in turn due to the insulating effect of the protein hindering the rapid transfer of electrons. These above results show the sensor was perfectly modified.

PEC Determination of CYFRA21-1. The fitting curve of this immunosensor was achieved under optimal experimental conditions, and the result is shown in Figure 3A. The optical flow response is linearly related to the logarithm of the Ag concentration (0.00001−500 ng·mL^{-1}); the equation of the fitting curve is $I = -607.2 - 87.24 \log c$ (ng·mL^{-1}) and the correlation coefficient is 0.9843 (Figure 3B). The limit of detection (LOD; n = 3) calculated according to the literature is about 0.0035 pg·mL^{-1}.

https://doi.org/10.1021/acs.analchem.2c01478
Anal. Chem. XXXX, XXX, XXX−XXX

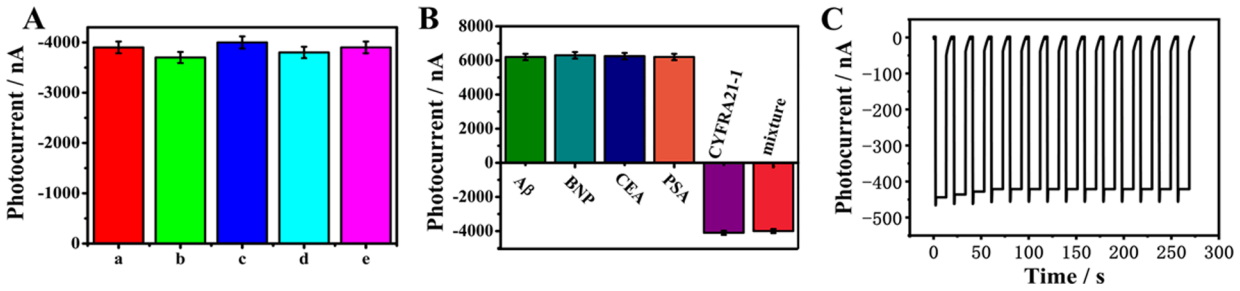

Figure 4. (A) Reproducibility test of the photoelectrochemical immunosensor. (B) Selectivity of the PEC sensing platform for CYFRA21-1 detection: CYFRA21-1, 0.5 ng·mL^{-1}; interferent, 50 ng·mL^{-1}. Mixture containing CYFRA21-1 (0.5 ng·mL^{-1}) and four interferents (the concentration of each interferent, 50 ng·mL^{-1}). (C) Stability test of the photoelectrochemical immunosensor. Error bars = SD (n = 3).

Reproducibility and Selectivity of the PEC Immunosensor. Good repeatability is the basic requirement of the sensor. Here, in order to study the repeatability of this immunosensor, under the uniform state, multiple electrodes were modified to measure the photocurrent. As depicted in Figure 4A, the relative standard deviation (RSD) of the sensor is less than 2.95%, which proves excellent repeatability of the immunosensor.

Selectivity is a key factor in evaluating the practicality of photoelectrochemical immunosensors. Here, Aβ (amyloid beta), BNP (brain natriuretic peptide), CEA (carcinoembryonic antigen), and PSA (prostate-specific antigen) were used to evaluate the selectivity of the PEC immunosensor (Figure 4B). The sensors constructed by the above single interference antigen (50 ng·mL^{-1}) all observed an anodic photocurrent. This phenomenon shows that these interferents cannot change the signal polarity of the sensor. A cathodic photocurrent was observed when the sensor platform was incubated with CYFRA21-1 (0.5 ng·mL^{-1}) without interference. In addition, the cathodic photocurrent was also observed in the mixed samples including CYFRA21-1 (0.5 ng·mL^{-1}) and all the above-mentioned interferents (the concentration of each interferent was 50 ng·mL^{-1}), and the value of the cathodic photocurrent was slightly smaller than that in the CYFRA21-1 sample. This meant that only CYFRA21-1 can generate a cathodic photocurrent, and the above-mentioned interferents caused an anodic photocurrent. The PEC response exhibited the RSD of 1.32%, which indicated that the PEC immunosensor developed has high selectivity.

In addition, to prove that photocurrent generated by the constructed sensor has good stability, the constructed sensor was detected for multiple periods. The current value of the sensor did not change much in multiple sensing cycles, which proves that the sensing platform has good stability.

Serum Sample Detection. In order to prove the practical value of the proposed PEC immunosensor, different concentrations (1, 5, and 10 ng·mL^{-1}) of the normal Ag solution were increased to serum samples. As depicted in Table S1, this means the recovery of this PEC sensor was between 97.20 and 102.1% and the RSD was 1.29−3.06%. Moreover, a comparison of our method and ELISA was added. The results are revealed in Table S2. As a result, the relative deviation of the two methods was in the range from −2.86 to 1.21%, suggesting that the PEC immunosensor was reliable and accurate for CYFRA21-1 detection.

4. CONCLUSION

An antigen-down photoelectrochemical immunosensor based on SnS_2 sensitized PTCA was successfully fabricated. Avidin-$CuInS_2$ and Ab-biotin were connected by the specific recognition of biotin and avidin. A conversion strategy of the photocurrent polarity before and after the modification of the marker was realized by the marker of avidin-$CuInS_2$, and the high sensitivity detection of CYFRA21-1 was completed. The immunosensor has a high sensitivity to CYFRA21-1 detection: the detection range is 0.00001−500 ng·mL^{-1} and the detection limit is 0.0035 pg·mL^{-1}. Compared with previous work (Table S3), the sensor has a wide detection range and a lower detection limit. Also, the immunosensor also has good stability and reproducibility. In clinical diagnosis, the PEC detection of CYFRA21-1 in non-small cell carcinoma samples provides a highly sensitive detection method, which has a certain application value for early diagnosis of lung cancer.

■ ASSOCIATED CONTENT

Supporting Information

The Supporting Information is available free of charge at https://pubs.acs.org/doi/10.1021/acs.analchem.2c01478.

Materials and reagents; apparatus; synthesis of SnS_2, PTCA, $CuInS_2$; optimization of detection conditions; photocurrent curves before and after marking; serum sample analysis; comparison of CYFRA21-1 detection methods (PDF)

■ AUTHOR INFORMATION

Corresponding Author

Xiang Ren − *Key Laboratory of Interfacial Reaction & Sensing Analysis in Universities of Shandong, School of Chemistry and Chemical Engineering and Collaborative Innovation Center for Green Chemical Manufacturing and Accurate Detection, University of Jinan, Jinan 250022 Shandong, China*; orcid.org/0000-0002-4321-4282; Phone: +86 531 82767862; Email: chem_renx@163.com

Authors

Jinhuan Zhang − *Key Laboratory of Interfacial Reaction & Sensing Analysis in Universities of Shandong, School of Chemistry and Chemical Engineering and Collaborative Innovation Center for Green Chemical Manufacturing and Accurate Detection, University of Jinan, Jinan 250022 Shandong, China*

Xiaodong Xue − *Shandong Academy of Environmental Sciences Co., Ltd., Jinan 250013 Shandong, China*

Yizhen Du − *Shandong Academy of Environmental Sciences Co., Ltd., Jinan 250013 Shandong, China*

Jinxiu Zhao − *Key Laboratory of Interfacial Reaction & Sensing Analysis in Universities of Shandong, School of*

https://doi.org/10.1021/acs.analchem.2c01478
Anal. Chem. XXXX, XXX, XXX−XXX

Chemistry and Chemical Engineering, University of Jinan, Jinan 250022 Shandong, China

Hongmin Ma − *Key Laboratory of Interfacial Reaction & Sensing Analysis in Universities of Shandong, School of Chemistry and Chemical Engineering and Collaborative Innovation Center for Green Chemical Manufacturing and Accurate Detection, University of Jinan, Jinan 250022 Shandong, China;* orcid.org/0000-0002-7061-8944

Qin Wei − *Key Laboratory of Interfacial Reaction & Sensing Analysis in Universities of Shandong, School of Chemistry and Chemical Engineering and Collaborative Innovation Center for Green Chemical Manufacturing and Accurate Detection, University of Jinan, Jinan 250022 Shandong, China;* orcid.org/0000-0002-3034-8046

Huangxian Ju − *Key Laboratory of Interfacial Reaction & Sensing Analysis in Universities of Shandong, School of Chemistry and Chemical Engineering and Collaborative Innovation Center for Green Chemical Manufacturing and Accurate Detection, University of Jinan, Jinan 250022 Shandong, China;* orcid.org/0000-0002-6741-5302

Complete contact information is available at: https://pubs.acs.org/10.1021/acs.analchem.2c01478

Notes

The authors declare no competing financial interest.

■ ACKNOWLEDGMENTS

This work was supported by the National Natural Science Foundation of Shandong Province (Nos. ZR2021QB120, ZR201911110108, ZR2020QB072) and the Special Foundation for Taishan Scholar Professorship of Shandong Province (Q.W. and H.J., No. ts201712052).

■ REFERENCES

(1) Barta, J. A.; Powell, C. A.; Wisnivesky, J. P. *Ann. Glob. Health.* **2019**, *85* (1), 8.
(2) Cao, M.; Chen, W. *Thorac. Cancer.* **2019**, *10* (1), 3−7.
(3) Herbst, R. S.; Morgensztern, D.; Boshoff, C. *Nature* **2018**, *553* (7689), 446−454.
(4) Yuan, M.; Huang, L. L.; Chen, J. H.; Wu, J.; Xu, Q. *Signal Transduct. Target. Ther.* **2019**, *4*, 61.
(5) Xu, R.; Du, Y.; Liu, L.; Fan, D.; Ren, X.; Liu, X.; Wei, Q.; Ju, H. *Microchim. Acta* **2021**, *188* (3), 75.
(6) Kumar, S.; Kumar, S.; Tiwari, S.; Augustine, S.; Srivastava, S.; Yadav, B. K.; Malhotra, B. D. *Sens. Actuators, B* **2016**, *235*, 1−10.
(7) Chen, M.; Hou, C.; Huo, D.; Yang, M.; Fa, H. *Analytical. Methods.* **2015**, *7* (22), 9466−9473.
(8) Qu, L.; Yang, L.; Li, Y.; Ren, X.; Wang, H.; Fan, D.; Wang, X.; Wei, Q.; Ju, H. *ACS Appl. Mater. Interfaces.* **2021**, *13* (4), 5795−5802.
(9) Liu, S.; Jia, Y.; Xue, J.; Li, Y.; Wu, Z.; Ren, X.; Ma, H.; Li, Y.; Wei, Q. *Sens. Actuators, B: Chem.* **2020**, *318*, 128278.
(10) Jia, Y.; Liu, S.; Du, Y.; Yang, L.; Liu, X.; Liu, L.; Ren, X.; Wei, Q.; Ju, H. *Anal. Chem.* **2020**, *92* (13), 9179−9187.
(11) Chen, Z.; Liang, R.; Guo, X.; Liang, J.; Deng, Q.; Li, M.; An, T.; Liu, T.; Wu, Y. *Biosens. Bioelectron* **2017**, *91*, 60−65.
(12) Zhang, J.; Ba, Y.; Liu, Q.; Zhao, L.; Wang, D.; Yang, H.; Kong, J. *J. Adv. Res.* **2020**, *22*, 77−84.
(13) Zhang, J.; Liu, Q.; Ba, Y.; Cheng, J.; Yang, H.; Cui, Y.; Kong, J.; Zhang, X. *Anal. Chim. Acta* **2020**, *1094*, 99−105.
(14) Hou, T.; Xu, N.; Wang, W.; Ge, L.; Li, F. *Anal. Chem.* **2018**, *90* (15), 9591−9597.
(15) Li, H.; Wang, J.; Wang, X.; Lin, H.; Li, F. *ACS Appl. Mater. Interfaces.* **2019**, *11* (18), 16958−16964.
(16) Song, X.; Hou, T.; Lu, F.; Wang, Y.; Liu, J.; Li, F. *Chem. Commun. (Camb)* **2020**, *56* (12), 1811−1814.
(17) Feng, J.; Li, F.; Li, X.; Ren, X.; Fan, D.; Wu, D.; Ma, H.; Du, B.; Zhang, N.; Wei, Q. *J. Mater. Chem. B* **2019**, *7* (7), 1142−1148.
(18) Wu, T.; Feng, J.; Zhang, S.; Liu, L.; Ren, X.; Fan, D.; Kuang, X.; Sun, X.; Wei, Q.; Ju, H. *Biosens. Bioelectron* **2020**, *169*, 112580.
(19) Lei, Y. M.; Wen, R. X.; Zhou, J.; Chai, Y. Q.; Yuan, R.; Zhuo, Y. *Anal. Chem.* **2018**, *90* (11), 6851−6858.
(20) Zhu, M. H.; Mu, X. M.; Deng, H. M.; Zhong, X.; Yuan, R.; Yuan, Y. L. *Chem. Commun. (Camb)* **2019**, *55* (65), 9622−9625.
(21) Tian, W.; Qiu, J.; Li, N.; Chen, D.; Xu, Q.; Li, H.; He, J.; Lu, J. *Nano Energy* **2021**, *86*, 106036.
(22) Zhang, Y. C.; Li, J.; Zhang, M.; Dionysiou, D. D. *Environ. Sci. Technol.* **2011**, *45* (21), 9324−9331.
(23) Chen, F. Z.; Han, D. M.; Chen, H. Y. *Anal. Chem.* **2020**, *92* (12), 8450−8458.
(24) Chen, G.; Qin, Y.; Jiao, L.; Huang, J.; Wu, Y.; Hu, L.; Gu, W.; Xu, D.; Zhu, C. *Anal. Chem.* **2021**, *93* (17), 6881−6888.
(25) Hinterding, S. O. M.; Mangnus, M. J. J.; Prins, P. T.; Jobsis, H. J.; Busatto, S.; Vanmaekelbergh, D.; de Mello Donega, C.; Rabouw, F. T. *Nano Lett.* **2021**, *21* (1), 658−665.
(26) Fan, G. C.; Shi, X. M.; Zhang, J. R.; Zhu, J. J. *Anal. Chem.* **2016**, *88* (21), 10352−10356.
(27) Haddour, N.; Chauvin, J.; Gondran, C.; Cosnier, S. *J. Am. Chem. Soc.* **2006**, *128*, 9693−9698.

Recommended by ACS

Sensitive Dual-Mode Biosensors for CYFRA21-1 Assay Based on the Dual-Signaling Electrochemical Ratiometric Strategy and "On–Off–On" PEC Method

Qingqing Zhang, Jinhua Chen, *et al.*
APRIL 20, 2021
ANALYTICAL CHEMISTRY
READ

Polydopamine with Tailorable Photoelectrochemical Activities for the Highly Sensitive Immunoassay of Tumor Markers

Xingxing Guan, Shuo Wu, *et al.*
APRIL 20, 2021
ANALYTICAL CHEMISTRY
READ

Dual-Mode Aptasensor Assembled by a WO_3/Fe_2O_3 Heterojunction for Paper-Based Colorimetric Prediction/Photoelectrochemical Multicomponent...

Jianli Sun, Jinghua Yu, *et al.*
JANUARY 12, 2021
ACS APPLIED MATERIALS & INTERFACES
READ

Self-Powered Cathodic Photoelectrochemical Aptasensor Comprising a Photocathode and a Photoanode in Microfluidic Analysis Systems

Jinhui Feng, Rongde Wu, *et al.*
APRIL 28, 2021
ANALYTICAL CHEMISTRY
READ

Get More Suggestions >